INTERNATIONAL JOURNAL OF
NUMERICAL ANALYSIS AND MODELING
Volume 4, Number 3-4, Pages 368–391

REDUCED ORDER MODELING OF SOME NONLINEAR STOCHASTIC PARTIAL DIFFERENTIAL EQUATIONS

JOHN BURKARDT, MAX D. GUNZBURGER, AND CLAYTON WEBSTER

Abstract. Determining accurate statistical information about outputs from ensembles of realizations is not generally possible whenever the input-output map involves the (computational) solution of systems of nonlinear partial differential equations (PDEs). This is due to the high cost of effecting each realization. Recently, in applications such as control and optimization that also require multiple solutions of PDEs, there has been much interest in reduced-order models (ROMs) that greatly reduce the cost of determining approximate solutions. We explore the use of ROMs for determining outputs that depend on solutions of stochastic PDEs. One is then able to cheaply determine much larger ensembles, but this increase in sample size is countered by the lower fidelity of the ROM used to approximate the state. In the contexts of proper orthogonal decomposition-based ROMs, we explore these counteracting effects on the accuracy of statistical information about outputs determined from ensembles of solutions.

Key Words. reduced order modeling, stochastic differential equations, brownian motion, monte carlo methods, finite element methods.

1. Introduction

Realistic simulations of complex systems governed by nonlinear partial differential equations must account for the "noisy" features of the modeled phenomena, such as material properties, coefficients, domain geometry, excitations and boundary data. "Noise" can be understood as uncertainties in the specification of the physical model; because of noise, the behavior of a complex system is at least partially unpredictable. A simulation can attempt to capture the noisy aspects of a system by describing the simulation input data as random fields. This turns the problem into a stochastic partial differential equation (SPDE). We will consider such problems, characterized by nonlinear partial differential equations, and for which the input data are not purely deterministic; for example, the coefficients or the right-hand-side of the partial differential equation may be regarded as sums of a deterministic and stochastic function.

For a given system, various stochastic perturbation techniques have been considered [1, 2, 4–6, 16, 19, 36, 64, 65]. This paper will focus on nonlinear SPDE's in which the stochastic inputs are modeled as white noise, i.e., they are not significantly correlated. The aim of our work is to efficiently determine statistical information

Received by the editors February 26, 2006 and, in revised form, April 25, 2006.
2000 *Mathematics Subject Classification.* 35R35, 49J40, 60G40.

about the random field $u = u(t, \mathbf{x}; \omega)$ from numerical approximations of the nonlinear SPDE driven by white noise:

$$\frac{\mathrm{d}u}{\mathrm{d}t} = Au - \gamma N(u) + g + \epsilon \frac{\mathrm{d}\mathbb{W}}{\mathrm{d}t}, \quad \mathbf{x} \in \mathcal{D}, \quad \omega \in \Omega, \quad t > 0. \tag{1.1}$$

Here $\mathcal{D} \subset \mathbb{R}^N$ is a convex, bounded and polygonal spatial domain, $(\Omega, \mathcal{F}, \mathbf{P})$ is a probability space described in section 2, and A is a linear second-order elliptic operator with deterministic coefficients, defined on a space of functions satisfying certain boundary conditions, $N(u)$ is a nonlinear function of the random process u, g represents a deterministic function and $\mathbb{W}$ denotes an infinite dimensional *Brownian motion* or *Wiener process*. The additive noise that appears in (1.1) is in the form of space-time Brownian white noise as described in section 2.1. The amplitudes of the noise and the nonlinearity are controlled by parameters ϵ and γ, respectively. Once the equation is reformulated into a weak form, the usual Galerkin finite element approach can be used to produce a discretized system suitable for solution on a computer.

Generally, obtaining precise statistics about ensembles of realizations of nonlinear SPDEs such as (1.1) entails a high cost in both memory and CPU. This cost is exhibited in many recent attempts on similar problems [9, 13, 26, 27]. Even with the use of reliable nonlinear solvers and carefully chosen solution schemes, these computations involve formidable work. Typical finite element codes may require the use of many thousands of degrees of freedom for the accurate simulation of deterministic PDEs. The situation becomes far worse when the same techniques are extended to SPDEs [20] for which multiple realizations are usually required.

It is natural to consider a reduced-order model (ROM), such as [10, 11]. A reduced-order model attempts to determine acceptable approximate solutions of a PDE while using very few degrees of freedom. One way to achieve this efficiency is for the models to use basis functions that are in some way intimately connected to the problem being solved. Once a low-dimensional reduced basis has been determined, it may be used in a new Galerkin system to solve related instances of the PDE. In this way, a ROM may be used to efficiently explore the behavior of large ensembles of PDE solutions. This is the kind of efficiency needed when attempting to compute realistic statistics from outputs of the SPDE.

There have been many reduced-order modeling techniques proposed; see [10, 11, 33, 37] and the references cited therein. The most popular reduced-order modeling approach for nonlinear PDEs is based on proper orthogonal decomposition (POD) analysis. POD begins with a set of $\widetilde{m}$ precomputed solutions of the equation, often called *snapshots*; these could be generated by evaluating the computational solution of a transient problem at many instants of time or over a range of values of the problem parameters. These solutions are presumably obtained using costly, large-scale, high-fidelity codes. The K-dimensional POD basis is then formed from the K eigenvectors corresponding to the dominant eigenvalues of the snapshot correlation matrix. This basis may then be used to construct a new finite element system of much reduced order, suitable for generating approximate solutions, at least within a limited range of the underlying snapshot data. POD-based model reduction has been applied with some success to several problems, most notably in fluid mechanics. For detailed discussions, one may consult [3, 7, 8, 10–12, 17, 25, 28, 29, 32–34, 43–48, 50–54, 59, 60, 62, 63].

The efficiency of a POD basis comes from its low dimension combined with its good approximating power. However, the ability of a POD-based basis to approximate the state of a system is totally dependent on the information contained in the

snapshot set. Certainly, a POD-based basis cannot contain more information than that contained in the snapshot set. Thus, crucial to the success of the POD-based approaches to model reduction is the generation of "good" snapshot sets, which manage to capture a wide range of system behaviors.

In order to present a standard approach, we focus on the case $\mathcal{D} = (0,1)\times(0,1) \subset \mathbb{R}^2$, $I := [t^1, T]$, a bounded interval of $\mathbb{R}$ and $Au = \Delta u = \left(\frac{\partial^2}{\partial x^2} + \frac{\partial^2}{\partial y^2}\right) u$ with homogeneous Dirichlet boundary conditions. However, much of our results and computations can be readily extended to higher spatial dimensions and more general second-order elliptic operators. An effort has been made to present most of this discussion using the familiar terminology from standard finite element methods for the numerical approximation of deterministic PDEs.

The paper is organized as follows: we first formulate the idea of a probability space, a Wiener process and Brownian motion in a plane half strip. Next, we discuss discrete Brownian white noise, the model nonlinear stochastic PDE and its finite element approximation. We then introduce the Monte Carlo-Galerkin finite element approximation by sampling input data for the nonlinear SPDE and then approximating the corresponding realization of the solution. Reduced-order models (ROMs) are generated and analyzed with respect to noise driven by the Brownian motion; computational error results are presented. Finally, some concluding remarks are given.

2. Preliminaries

We begin by recalling the mathematical formulation of a probability space $(\Omega, \mathcal{F}, \mathbf{P})$, where Ω, $\mathcal{F}$ and $\mathbf{P}$ are the set of random events, the minimal σ-algebra of subsets of Ω, and the probability measure, respectively. We define $D \subset \mathbb{R}^N$ to be a bounded spatial domain.

If X is a real random variable in $(\Omega, \mathcal{F}, \mathbf{P})$ with $X \in L^1(\Omega)$, we denote its expected value by

$$\mathbf{E}[X] = \int_\Omega X(\omega)\mathbf{P}(\mathrm{d}\omega) = \int_{\mathbb{R}} x\mu(\mathrm{d}x). \tag{2.1}$$

Here μ is the distribution probability measure for X, defined on the Borel set $\mathcal{B}$ of $\mathbb{R}$, given by

$$\mu(\mathcal{B}) = \mathbf{P}\left(X^{-1}(\mathcal{B})\right). \tag{2.2}$$

We will assume that $\mu(\mathcal{B})$ is absolutely continuous with respect to Lebesque measure; then there exists a density function for X, $\rho : \mathbb{R} \to \mathbb{R}^+$, such that

$$\mathbf{E}[X] = \int_{\mathbb{R}} x\rho(x)\mathrm{d}x. \tag{2.3}$$

Next, we define what is meant by a measurable *stochastic* and *Wiener* process and formally explain the concept of a Brownian motion on a plane half-strip (otherwise known as a Brownian sheet):

Definition 2.1. *An (N,d)-valued stochastic process $\mathbb{U}(\mathbf{z}) = \left\{\mathbb{U}(\mathbf{z}); \mathbf{z} \in \mathbb{R}^N_+\right\} = \{(\mathbb{U}_1(\mathbf{z}), \ldots, \mathbb{U}_d(\mathbf{z}))\}_{\mathbf{z}\in\mathbb{R}^N_+}$, defined on a probability space $(\Omega, \mathcal{F}, \mathbf{P})$, is measurable if*

$$\mathbb{U} : \Omega \times \mathbb{R}^N_+ \to \mathbb{R}^d$$

is $\mathcal{F} \times \mathcal{B}(\mathbb{R}^N_+)$ measurable.

Notice that when $N = 1$, $\mathbb{U}$ is just an $\mathbb{R}^d$-valued stochastic process.

Definition 2.2. *An $\mathbb{R}$-valued stochastic process $W(t) = \{W(t)\}_{t\in\mathbb{R}^1_+}$ is called a Brownian motion or Wiener process if*

- $W_0 = 0$ *a.s.,*
- $W_t - W_s$ *is* $N(0, t-s)$[1] *for all* $t \geq s \geq 0$
- *for all times* $0 < t_1 < t_2 < \cdots < t_n$*, the random variables* $W_{t_1}, W_{t_2} - W_{t_1}, \ldots, W_{t_n} - W_{t_{n-1}}$ *are independent ("independent increments").*

Notice that

$$\mathbf{E}(W_t) = 0, \quad \mathbf{E}(W_t^2) = t \text{ for each } t \geq 0.$$

We complete this section by defining Brownian motion on a plane half strip or Brownian sheet $\mathbb{W}(t, \mathbf{z})$, $t \in \mathbb{R}^1_+$ and $\mathbf{z} \in \mathbb{R}^{N-1}_+$.

Definition 2.3. *Let $\mathbb{W}(t, \mathbf{z}) = \{\mathbb{W}(t, \mathbf{z})\}_{t\in\mathbb{R}^1_+, \mathbf{z}\in\mathbb{R}^{N-1}_+}$ denote an (N, d) Brownian sheet. That is, $\mathbb{W}$ is the N-parameter Gaussian random field with values in $\mathbb{R}^d$, its mean-function is zero, and its covariance function is given by the following: for all $t, s \in \mathbb{R}^1_+$ and $\mathbf{z}, \mathbf{w} \in \mathbb{R}^{N-1}_+$ and all $1 \leq i, j \leq d$,*

$$\mathbf{E}\left(\mathbb{W}_i(t, \mathbf{z}) \cdot \mathbb{W}_j(s, \mathbf{w})\right) = \begin{cases} (t \wedge s) \times \displaystyle\prod_{k=1}^{N} (z_k \wedge w_k), & \text{if } i = j \\ 0, & \text{if } i \neq j \end{cases}$$

We have written $\mathbb{W}(t, \mathbf{z})$ in vector form as $\{(\mathbb{W}_1(t, \mathbf{z}), \ldots, \mathbb{W}_d(t, \mathbf{z}))\}_{t\in\mathbb{R}^1_+, \mathbf{z}\in\mathbb{R}^{N-1}_+}$, as is customary. When $N = 1$, $\mathbb{W}$ is just Brownian motion in $\mathbb{R}^d$.

Now consider the three-dimensional Gaussian white noise

$$\Delta\mathbb{W}(t, \mathbf{x}) = \frac{\partial^3 \mathbb{W}}{\partial t \partial x_1 \partial x_2}(t, \mathbf{x}; \omega), \quad \mathbf{x} = (x_1, x_2) \in D \subset \mathbb{R}^2$$

where $\mathbb{W}(t, \mathbf{x})$ is Brownian motion on a half plane or a Brownian sheet satisfying, for $t, s \in \mathbb{R}^1_+$ and $\mathbf{x}, \mathbf{y} \in \mathcal{D}$:

$$\begin{aligned} \mathbf{E}\left(\Delta\mathbb{W}(t, \mathbf{x}) \cdot \Delta\mathbb{W}(s, \mathbf{y})\right) &= \delta(t - s) \times \delta(\mathbf{x} - \mathbf{y}) \\ &= \delta(t - s) \times \delta(x_1 - y_1) \times \delta(x_2 - y_2) \end{aligned} \tag{2.4}$$

with δ the usual Dirac δ-function. According to [1], application of standard finite element techniques requires that $\Delta\mathbb{W}(t, \mathbf{x}) = \Delta\mathbb{W}(t, x_1, x_2)$ be modeled by the piecewise constant random process given in the following section.

2.1. The approximation of Brownian white noise. Following [1, 20, 65], we regularize the noise through discretization. For simplicity, we use a uniform discretization $0 = t^1 < t^2 < \cdots < t^n < \cdots < t^{\widetilde{N}} = T$ of the time interval $[t^1, T]$ given by

$$t^{n+1} = t^1 + n\Delta t, \quad t > 1$$

with $\Delta t = (T - t_1)/\widetilde{N}$, for some integer $\widetilde{N}$ large enough so that $\Delta t \in (0, 1)$. Likewise, we consider a uniform finite element triangulation $\{\tau_j\}_{j=1}^{\widetilde{M}}$ of the square $\mathcal{D}$ characterized by the parameter h, which we take to be the longest side of any triangle. We denote by $\Delta\tau$ the area of any of the finite elements.

[1] $N(0, t-s)$ is the zero-mean Gaussian (or normal) distribution with variance $t - s$

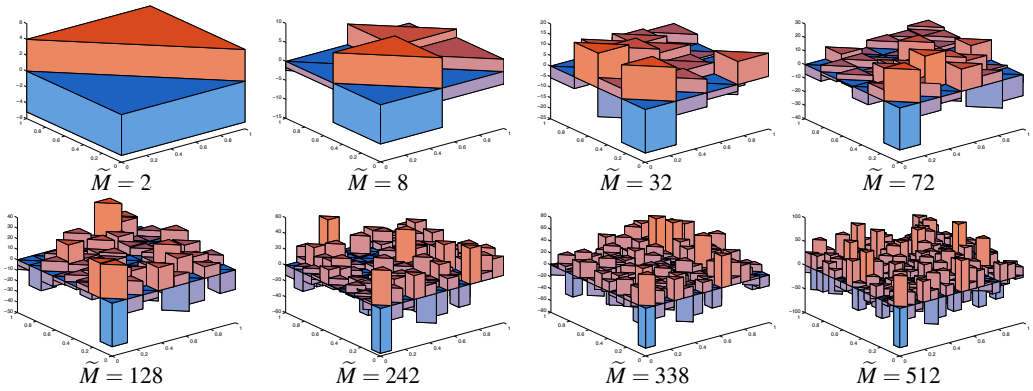

FIGURE 1. Piecewise constant approximation for the noise $\Delta\widehat{\mathbb{W}}(t,\mathbf{x}) = c_{\widetilde{N}\widetilde{M}} \sum_{i=1}^{\widetilde{N}} \sum_{j=1}^{\widetilde{M}} \eta_{ij}\chi_i(t)\chi_j(\mathbf{x})$ at the final time $T = 1$ over a uniform finite element triangulation. The number of elements ranges from $\widetilde{M} = 2$ to $\widetilde{M} = 512$.

Using the finite element triangulation $\{\tau_j\}_{j=1}^{\widetilde{M}}$ of D, and guided by Lemma 2.4, a "reasonable" piecewise constant approximation of the noise is given by

$$\Delta\widehat{\mathbb{W}}(t,\mathbf{x}) = \frac{\partial^3 \widehat{\mathbb{W}}}{\partial t \partial x_1 \partial x_2}(t,\mathbf{x};\omega) = c_{\widetilde{N}\widetilde{M}} \sum_{i=1}^{\widetilde{N}} \sum_{j=1}^{\widetilde{M}} \eta_{ij}(\omega)\chi_i(t)\chi_j(\mathbf{x}), \tag{2.5}$$

where

$$c_{\widetilde{N}\widetilde{M}} = \frac{1}{\sqrt{\Delta t}\sqrt{\Delta\tau}}$$

and, for $i = 1, 2, \ldots, \widetilde{N} - 1$, $j = 1, 2, \ldots, \widetilde{M} - 1$, $\eta_{ij} \in N(0,1)$ is independently and identically distributed (iid),

$$\sqrt{\Delta t}\sqrt{\Delta\tau}\,\eta_{ij} = \int_{t^i}^{t^{i+1}} \int_{\tau_j} \mathrm{d}\mathbb{W}(t,\mathbf{x}),$$

$$\chi_i(t) = \begin{cases} 1, & \text{if } t^i \le t < t^{i+1}, \\ 0, & \text{otherwise} \end{cases} \qquad \text{and} \qquad \chi_j(\mathbf{x}) = \begin{cases} 1, & \text{if } \mathbf{x} \in \tau_j, \\ 0, & \text{otherwise}. \end{cases}$$

That is, $\chi_i(t)$ is the characteristic function for the ith time interval and $\chi_j(\mathbf{x})$ is the characteristic function for the jth finite element. For an arbitrary i and j, the discrete analog of (2.4) for the piecewise constant approximation to $\Delta\widehat{\mathbb{W}}$ is given by

$$\mathbf{E}\left(\Delta\widehat{\mathbb{W}}(t,\mathbf{x}) \cdot \Delta\widehat{\mathbb{W}}(s,\mathbf{y})\right) = \begin{cases} \dfrac{1}{\Delta t} \times \dfrac{1}{\Delta\tau}, & \text{if } t^i \le t, s < t^{i+1} \text{ and } \mathbf{x}, \mathbf{y} \in \tau_j, \\ 0, & \text{otherwise} \end{cases}$$

Therefore,

$$\lim_{\widetilde{N},\widetilde{M}\to\infty} \mathbf{E}\left(\Delta\widehat{\mathbb{W}}(t,\mathbf{x}) \cdot \Delta\widehat{\mathbb{W}}(s,\mathbf{y})\right) = \delta(t-s) \times \delta(\mathbf{x}-\mathbf{y})$$

as required. In Figure 2.1, some sample realizations of the piecewise constant approximation of the three-parameter white noise are displayed for $\Delta t = 1$ and various values of $\widetilde{M}$ at the final time $T = 1$.

Similarly to [1], we have the following result for a nonrandom function $f(t, \mathbf{x})$.

Lemma 2.4. *Let f be a nonrandom function and Lipschitz continuous on $[0, T] \times [0, 1] \times [0, 1]$. In particular, assume that there is a positive constant $\gamma \geq 0$ such that $|f(t, \mathbf{x}) - f(s, \mathbf{y})| \leq \gamma (|t - s| + \|\mathbf{x} - \mathbf{y}\|)$ for $(t, \mathbf{x}), (s, \mathbf{y}) \in [0, T] \times [0, 1] \times [0, 1]$. Then*

$$\mathbf{E}\left[\int_0^T \int_{\mathcal{D}} f(t, \mathbf{x}) d\mathbb{W}(t, \mathbf{x}) - \int_0^T \int_{\mathcal{D}} f(t, \mathbf{x}) d\widehat{\mathbb{W}}(t, \mathbf{x})\right]^2 \leq 2T\gamma^2 \left((\Delta t)^2 + h^2\right).$$

Proof. The proof is as follows:

$$\begin{aligned}
&\mathbf{E}\left[\int_0^T \int_{\mathcal{D}} f(t, \mathbf{x}) \mathrm{d}\mathbb{W}(t, \mathbf{x}) - \int_0^T \int_{\mathcal{D}} f(t, \mathbf{x}) \mathrm{d}\widehat{\mathbb{W}}(t, \mathbf{x})\right]^2 \\
&= \mathbf{E}\left[\sum_{i=1}^{\widetilde{N}} \sum_{j=1}^{\widetilde{M}} \int_{t^i}^{t^{i+1}} \int_{\tau_j} f(t, \mathbf{x}) \mathrm{d}\mathbb{W}(t, \mathbf{x})\right. \\
&\quad \left. - \sum_{i=1}^{\widetilde{N}} \sum_{j=1}^{\widetilde{M}} \int_{t^i}^{t^{i+1}} \int_{\tau_j} f(s, \mathbf{y}) \left(\frac{1}{\Delta t \Delta \tau} \int_{t^i}^{t^{i+1}} \int_{\tau_j} \mathrm{d}\mathbb{W}(t, \mathbf{x})\right) \mathrm{d}\mathbf{y}\mathrm{d}s\right]^2 \\
&= \mathbf{E}\left[\sum_{i=1}^{\widetilde{N}} \sum_{j=1}^{\widetilde{M}} \int_{t^i}^{t^{i+1}} \int_{\tau_j} \left(f(t, \mathbf{x}) - \frac{1}{\Delta t \Delta \tau} \int_{t^i}^{t^{i+1}} \int_{\tau_j} f(s, \mathbf{y}) \mathrm{d}\mathbf{y}\mathrm{d}s\right) \mathrm{d}\mathbb{W}(t, \mathbf{x})\right]^2 \\
&= \sum_{i=1}^{\widetilde{N}} \sum_{j=1}^{\widetilde{M}} \int_{t^i}^{t^{i+1}} \int_{\tau_j} \left(f(t, \mathbf{x}) - \frac{1}{\Delta t \Delta \tau} \int_{t^i}^{t^{i+1}} \int_{\tau_j} f(s, \mathbf{y}) \mathrm{d}\mathbf{y}\mathrm{d}s\right)^2 \mathrm{d}\mathbf{x}\mathrm{d}t \\
&= \sum_{i=1}^{\widetilde{N}} \sum_{j=1}^{\widetilde{M}} \int_{t^i}^{t^{i+1}} \int_{\tau_j} \left(\frac{1}{\Delta t \Delta \tau} \int_{t^i}^{t^{i+1}} \int_{\tau_j} (f(t, \mathbf{x}) - f(s, \mathbf{y})) \mathrm{d}\mathbf{y}\mathrm{d}s\right)^2 \mathrm{d}\mathbf{x}\mathrm{d}t \\
&\leq \frac{\gamma^2}{(\Delta t \Delta \tau)^2} \sum_{i=1}^{\widetilde{N}} \sum_{j=1}^{\widetilde{M}} \int_{t^i}^{t^{i+1}} \int_{\tau_j} \left(\int_{t^i}^{t^{i+1}} \int_{\tau_j} (|t - s| + \|\mathbf{x} - \mathbf{y}\|) \mathrm{d}\mathbf{y}\mathrm{d}s\right)^2 \mathrm{d}\mathbf{x}\mathrm{d}t \\
&\leq \frac{\gamma^2}{(\Delta t \Delta \tau)^2} \sum_{i=1}^{\widetilde{N}} \sum_{j=1}^{\widetilde{M}} \int_{t^i}^{t^{i+1}} \int_{\tau_j} \left(\int_{t^i}^{t^{i+1}} \int_{\tau_j} (\Delta t + h) \mathrm{d}\mathbf{y}\mathrm{d}s\right)^2 \mathrm{d}\mathbf{x}\mathrm{d}t \\
&= \gamma (\Delta t + h)^2 \sum_{i=1}^{\widetilde{N}} \sum_{j=1}^{\widetilde{M}} \int_{t^i}^{t^{i+1}} \int_{\tau_j} \mathrm{d}\mathbf{x}\mathrm{d}t \leq 2T\gamma^2 \left((\Delta t)^2 + h^2\right).
\end{aligned}$$

□

3. The model nonlinear stochastic partial differential equation and its finite element approximation

In this section we discuss the formulation of the nonlinear stochastic PDE and its finite element approximation. Let $\mathcal{D} = \mathcal{D}_1 \times \mathcal{D}_2$ be a bounded region in $\mathbb{R}^2$ whose boundary is denoted $\partial\mathcal{D}$; let T denote a positive constant. Denote $\mathbf{x} = (x_1, x_2) \in \mathcal{D}$ such that $x_1 \in \mathcal{D}_1$ and $x_2 \in \mathcal{D}_2$. Let ϵ denote the given (constant)

perturbation parameter that measures the amplitude of the space-time white noise $\frac{\partial^3 \mathbb{W}}{\partial t \partial x_1 \partial x_2}(t, \mathbf{x}; \omega)$. Furthermore, let g be a deterministic function. We consider the model nonlinear stochastic partial differential equation on a bounded interval $I := (0, T) \subset \mathbb{R}$ as follows: find $u : \bar{I} \times \mathcal{D} \to \mathbb{R}$ such that

$$\begin{cases} \dfrac{\partial u}{\partial t}(t, \mathbf{x}) - \Delta u(t, \mathbf{x}) + \gamma N(u(t, \mathbf{x})) = g(t, \mathbf{x}) + \epsilon \dfrac{\partial^3 \mathbb{W}}{\partial t \partial x_1 \partial x_2}(t, \mathbf{x}; \omega), \text{ in } I \times \mathcal{D} \\ u(t, \mathbf{x}) = 0, \text{ on } \partial\mathcal{D} \\ u(0, \mathbf{x}) = 0, \text{ in } \mathcal{D}, \end{cases} \tag{3.1}$$

where $N : \bar{I} \times \mathcal{D} \to \mathbb{R}$ is a nonlinear function of $u(t, \mathbf{x})$ and γ denotes the strength of the nonlinearity. Setting $\epsilon = 0$ reduces (3.1) to a deterministic PDE for which standard reduced-order methods apply. Similarly, setting $\gamma = 0$ reduces (3.1) to a linear stochastic PDE.

Generally, when discussing the stochastic process $u(t, \mathbf{x}; \omega)$, we will omit the explicit dependence on the probability space Ω, treating each realization as a deterministic PDE, unless it will be useful for clarity's sake to make this dependence explicit.

3.1. The Nonlinear Monte Carlo Finite Element Method. The Monte Carlo Finite Element Method is a natural choice for handling a stochastic PDE. If the aim is to compute a functional of the solution u, such as its expected value, one would try to approximate the integral $\mathbf{E}(u(\cdot\,; \omega))$ numerically by sample averages of iid realizations corresponding to sample white noise functions. In fact, all the statistics we are interested are really integrals of a function $u(\cdot\,; \omega)$ over Ω.

We begin with a variational formulation, to define a finite element method suitable for producing approximate solutions of (3.1); of course, many other methods could also be used. A variational formulation of (3.1) is the following: find $u(t, \cdot)$, $t \in I$, such that

$$\begin{cases} \displaystyle\int_{\mathcal{D}} u(t, \mathbf{x}) \phi(\mathbf{x}) \mathrm{d}\mathcal{D} + \int_0^T \int_{\mathcal{D}} \{\nabla u \cdot \nabla \phi\} \mathrm{d}\mathcal{D} \mathrm{d}s \\ \qquad\qquad + \gamma \displaystyle\int_0^T \int_{\mathcal{D}} N(u(s, \mathbf{x})) \phi(\mathbf{x}) \mathrm{d}\mathcal{D} \mathrm{d}s \\ \qquad\qquad = \displaystyle\int_0^T \int_{\mathcal{D}} g(s, \mathbf{x}) \phi(\mathbf{x}) \mathrm{d}\mathcal{D} \mathrm{d}s + \epsilon \int_0^T \int_{\mathcal{D}} \phi(\mathbf{x}) \mathrm{d}\mathbb{W}(s, \mathbf{x}), \\ \qquad u(0, \mathbf{x}) = 0, \text{ in } \mathcal{D}. \end{cases} \tag{3.2}$$

for all $\phi \in H_0^1(\mathcal{D})$. The last integral in (3.2) is understood in the Itô sense.

The semi-discretization in space leads to the following problem: find $u(t, \cdot) \in H_0^1(\mathcal{D})$, $t \in I$, such that

$$(u_t, \phi(\mathbf{x}))_{L^2(\mathcal{D})} + \mathscr{B}(u, \phi) = \mathscr{F}(\phi) \quad \text{for all } \phi \in H_0^1(\mathcal{D}) \tag{3.3}$$

where

$$\begin{aligned} \mathscr{B}(u, \phi) &= \int_{\mathcal{D}} \nabla u \cdot \nabla \phi \mathrm{d}\mathcal{D} + \gamma \int_{\mathcal{D}} N(u(t, \mathbf{x})) \phi(\mathbf{x}) \mathrm{d}\mathcal{D} \\ &= (\nabla u, \nabla \phi)_{L^2(\mathcal{D})} + (N(u), \phi)_{L^2(\mathcal{D})} \end{aligned} \tag{3.4}$$

and

$$\begin{aligned}\mathscr{F}(\phi) &= \int_{\mathcal{D}} \left(g(t,\mathbf{x}) + \epsilon \frac{\partial^3 \widehat{\mathbb{W}}}{\partial t \partial x_1 \partial x_2}(t,\mathbf{x};\omega) \right) \phi(\mathbf{x}) \mathrm{d}\mathcal{D} \\ &= (g,\phi)_{L^2(\mathcal{D})} + \left(\Delta\widehat{\mathbb{W}}, \phi \right)_{L^2(\mathcal{D})}\end{aligned} \tag{3.5}$$

respectively. We note that $u_t := \frac{\partial u}{\partial t}$.

For each realization of the piecewise constant noise $\Delta\widehat{\mathbb{W}}$, a realization of the approximate solution is computed, using a time-marching scheme such as the standard backward Euler-Galerkin finite element method. Linearization is accomplished by a Newton or Quasi-Newton approach. Here it will be helpful to write the solution as $u(\cdot\,;\omega)$ to emphasize the dependence on the probability space $(\Omega, \mathscr{F}, \mathbf{P})$. The challenge is that we do not know $u(\cdot\,;\omega)$, as this remains an unknown quantity of interest. Hence, we formulate a solution procedure that does not require knowledge of a functional form for $u(\cdot\,;\omega)$ for all $\omega \in \Omega$.

This method is as follows:

(1) Choose the number of realizations $M \in \mathbb{N}_+$ and a piecewise continuous finite element approximating space of $\mathcal{D}$, S_0^h.

(2) For each $k = 1, \ldots, M$, sample iid realizations of the piecewise constant noise $\Delta\widehat{\mathbb{W}}(\cdot\,;\omega_k)$ and produce approximations $u^h(\cdot\,;\omega_k) \in S_0^h$ such that

$$\begin{aligned}&(u_t^h(\cdot\,;\omega_k), \phi^h)_{L^2(\mathcal{D})} + \widetilde{\mathscr{B}}(u^h(\cdot\,;\omega_k), \phi^h) \\ &= \widetilde{\mathscr{F}}(\phi^h) = \left(g(\cdot) + \epsilon \Delta\widehat{\mathbb{W}}(\cdot\,;\omega_k), \phi^h \right)_{L^2(\mathcal{D})} \quad \forall \phi^h \in S_0^h\end{aligned}$$

where $\widetilde{\mathscr{B}}$ and $\widetilde{\mathscr{F}}$ are the stochastic forms of (3.4) and (3.5) respectively, defined by

$$\forall \omega \in \Omega : \widetilde{\mathscr{B}}(\phi_1, \phi_2) = \mathscr{B}(\phi_1, \phi_2; \omega) \quad \forall \phi_1, \phi_2 \in H_0^1(\mathcal{D})$$

and

$$\widetilde{\mathscr{F}}(\phi_2) = \mathscr{F}(\phi_2; \omega) \quad \forall \phi_2 \in H_0^1(\mathcal{D}).$$

Once we have fixed $\omega = \omega_k$, the problem is completely deterministic, and may be solved by standard methods.

(3) Approximate $\mathbf{E}(u)$ by the sampling average:

$$\overline{\mathbf{E}}(u^h; M) = \frac{1}{M} \sum_{k=1}^{M} u^h(\cdot\,;\omega_k) \tag{3.6}$$

We only consider the case where S_0^h is fixed for all realizations, in particular, we have fixed the triangulation $\{\tau_j\}$ of $\mathcal{D}$ and employ a backward-Euler scheme for the time discretization.

The computational error for the finite element approximation to the stochastic PDE may be considered in two parts

$$\mathbf{E}(u) - \overline{\mathbf{E}}(u^h; M) = \big(\mathbf{E}(u) - \mathbf{E}(u^h)\big) + \big(\mathbf{E}(u^h) - \overline{\mathbf{E}}(u^h; M)\big) = \mathscr{E}_T^h + \mathscr{E}_{T,S}^h \tag{3.7}$$

The characteristic size h, and the backward-Euler method control the space-time discretization error $\mathscr{E}_T^h$, while the number of realizations, N of u^h, controls the statistical error $\mathscr{E}_{T,S}^h$. A comprehensive study of such statistical error was completed by [5].

4. Reduced-order modeling for the nonlinear stochastic partial differential equation

In this section, we briefly describe the reduced-order model (ROM) for the nonlinear stochastic PDE (3.1). In Section 5, we will use a concrete example to exhibit the relative accuracy and efficiency of the ROM compared to the standard FEM approach. The generation of the reduced-order model requires a set of snapshot solution vectors; see section 5.1 for a discussion of snapshots.

4.1. POD reduced-order bases. Given a discrete set of snapshot vectors $W = \{\vec{w}_n\}_{n=1}^N$ belonging to $\mathbb{R}^J$, we form the $J \times N$ snapshot matrix $\mathbb{A}$ whose columns are the snapshot vectors $\vec{w}_n$:

$$\mathbb{A} = \begin{pmatrix} \vec{w}_1 & \vec{w}_2 & \cdots & \vec{w}_N \end{pmatrix}.$$

Let

$$\mathbb{U}^T \mathbb{A} \mathbb{V} = \begin{pmatrix} \Sigma & 0 \\ 0 & 0 \end{pmatrix},$$

where $\mathbb{U}$ and $\mathbb{V}$ are $J \times J$ and $N \times N$ orthogonal matrices, respectively, and $\Sigma = \text{diag}(\sigma_1, \ldots, \sigma_{\widetilde{M}})$ with $\sigma_1 \geq \sigma_2 \geq \cdots \geq \sigma_{\widetilde{M}}$ be the singular value decomposition of $\mathbb{A}$. Here, $\widetilde{M}$ is the rank of $\mathbb{A}$, i.e., the dimension of the snapshot set W, which would be less than N whenever the snapshot set is linearly dependent. It can easily be shown that if

$$\mathbb{U} = \begin{pmatrix} \vec{\Phi}_1 & \vec{\Phi}_2 & \cdots & \vec{\Phi}_J \end{pmatrix} \qquad \text{and} \qquad \mathbb{V} = \begin{pmatrix} \vec{\psi}_1 & \vec{\psi}_2 & \cdots & \vec{\psi}_N \end{pmatrix},$$

then

$$\mathbb{A}\vec{\psi}_i = \sigma_i \vec{\Phi}_i \qquad \text{and} \qquad \mathbb{A}^T \vec{\Phi}_i = \sigma_i \vec{\psi}_i \qquad \text{for } i = 1, \ldots, \widetilde{M}$$

so that also

$$\mathbb{A}^T \mathbb{A}\vec{\psi}_i = \sigma_i^2 \vec{\psi}_i \qquad \text{and} \qquad \mathbb{A}\mathbb{A}^T \vec{\Phi}_i = \sigma_i^2 \vec{\Phi}_i \qquad \text{for } i = 1, \ldots, \widetilde{M}$$

so that σ_i^2, $i = 1, \ldots, \widetilde{M}$, are the nonzero eigenvalues of $\mathbb{A}^T\mathbb{A}$ (and also of $\mathbb{A}\mathbb{A}^T$) arranged in nondecreasing order. The matrix $\mathbb{C} = \mathbb{A}^T\mathbb{A}$ is simply the correlation matrix of the snapshot vectors $W = \{\vec{w}_n\}_{n=1}^N$, i.e., we have that $\mathbb{C}_{mn} = \vec{w}_m^T \vec{w}_n$.

In the reduced-order modeling context, given a set of snapshots $W = \{\vec{w}_n\}_{n=1}^N$ belonging to $\mathbb{R}^J$, the POD reduced basis of dimension $K \leq N < J$ is the set $\{\vec{\Phi}_k\}_{k=1}^K$ of vectors also belonging to $\mathbb{R}^J$ consisting of the first K left singular vectors of the snapshot matrix $\mathbb{A}$. Thus, one can determine the POD basis by computing the (partial) singular value decomposition of the $J \times N$ matrix $\mathbb{A}$. Alternately, one can compute the (partial) eigensystem $\{\sigma_k^2, \vec{\psi}_i\}_{i=1}^K$ of the $N \times N$ correlation matrix $\mathbb{C} = \mathbb{A}^T\mathbb{A}$ and then set $\vec{\Phi}_k = \frac{1}{\sigma_k}\mathbb{A}\vec{\psi}_k$, $k = 1, \ldots, K$.

The K-dimensional POD basis has the obvious property of orthonormality. It also has several other important properties which we now mention. Let $\{\vec{s}_k\}_{k=1}^K$ be an arbitrary set of K orthonormal vectors in $\mathbb{R}^J$ and let $\Pi\vec{w}$ denote the projection of a vector $\vec{w} \in \mathbb{R}^J$ onto the subspace spanned by that set. Further, let

$$\mathcal{E}(\vec{s}_1, \ldots, \vec{s}_K) = \sum_{n=1}^N |\vec{w}_n - \Pi\vec{w}_n|^2,$$

i.e., $\mathcal{E}$ is the sum of the squares of the error between each snapshot vector $\vec{w}_n$ and its projection $\Pi\vec{w}_n$ onto the span of $\{\vec{s}_k\}_{k=1}^K$. Then, it can be shown that

$$\left\{ \begin{array}{l} \textit{the POD basis } \{\vec{\Phi}_k\}_{k=1}^K \textit{ minimizes } \mathcal{E} \textit{ over all possible} \\ K\textit{-dimensional orthonormal sets in } \mathbb{R}^J. \end{array} \right. \tag{4.1}$$

In fact, the POD basis corresponding to a set of snapshots $W = \{\vec{w}_n\}_{n=1}^N$ is often defined by (4.1), and then its relation to the singular value decomposition of the matrix $\mathbb{A}$, or to the eigenvalue decomposition of $\mathbb{A}^T\mathbb{A}$, are derived properties. We note that $\mathcal{E}(\vec{\Phi}_1, \ldots, \vec{\Phi}_K)$ is referred to as the "POD energy" or "error in the POD basis." Also, it can be shown that

$$\mathcal{E}(\vec{\Phi}_1, \ldots, \vec{\Phi}_K) = \sum_{k=K+1}^{\widetilde{M}} \sigma_k^2, \tag{4.2}$$

i.e., the error in the POD basis is simply the sum of the squares of the singular values corresponding to the neglected POD modes.

Another property of the POD basis is given as follows:

$$\begin{cases} \textit{the POD basis } \{\vec{\Phi}_k\}_{k=1}^K \textit{ solves the sequence of problems:} \\ \textit{for } k = 1, \ldots, K, \qquad \max\limits_{\vec{s}_k \in \mathbb{R}^J} \sum\limits_{n=1}^{N} \left(\vec{w}_n^T \vec{s}_k\right)^2 \\ \textit{subject to } |\vec{s}_k| = 1 \textit{ and } \vec{s}_j^T \vec{s}_k = 0 \textit{ for } j = 1, \ldots, k-1. \end{cases} \tag{4.3}$$

Again, (4.3) is often used to define the POD basis and then its relation to the singular value decomposition and (4.1) are noted as derived properties.

The singular values of the snapshot matrix may be used to determine a practical value for the dimension K of the POD basis. Indeed, it is a simple matter to show that if one requires the error in the POD basis to be less than some prescribed tolerance δ, i.e., that

$$\mathcal{E}(\vec{\Phi}_1, \ldots, \vec{\Phi}_K) \leq \delta,$$

then one need only

$$\textit{choose } K \textit{ to be the smallest integer such that} \qquad \frac{\sum_{k=1}^K \sigma_k^2}{\sum_{k=1}^{\widetilde{M}} \sigma_k^2} \geq 1 - \delta.$$

The usefulness of POD-based reduced-order modeling is derived from the observation that in many settings one finds that, even if δ is chosen to be relatively small, e.g., 0.01, one can still be able to use a basis of low order K; K is usually much smaller than $\widetilde{M}$ and might be of order 10 or so.

For reduced-order modeling applications, the snapshot vectors are coefficient vectors in the expansion of the finite element approximation of the stochastic process evaluated at different instants in time. Thus, to each snapshot vector $\vec{w}_n$, $n = 1, \ldots, N$, there corresponds a finite element function

$$w_n(\mathbf{x}) = \sum_{j=1}^{J} \mathbf{w}_{j,n} \phi_j(\mathbf{x}) \in S_0^h, \tag{4.4}$$

where $\mathbf{w}_{j,n}$ denotes the j-th component of the vector $\vec{w}_n$ and $\phi_j(\mathbf{x}) \in V_0^h$ denotes the j-th finite element basis function. One can define a POD basis with respect to functions instead of vectors, i.e., we could start with a snapshot set $W = \{w_n(\mathbf{x})\}_{n=1}^N$ consisting of finite element functions belonging to S_0^h. Then, instead of (4.3), one could define the POD basis $\{\Phi_k(\mathbf{x}) \in V_0^h\}_{k=1}^K$ to be the solution of the sequence of problems: *for* $k = 1, \ldots, K$,

$$\max_{s_k(\mathbf{x}) \in V_0^h} \sum_{n=1}^{N} \langle w_n, s_k \rangle_0^2$$

subject to $\|s_k(\mathbf{x})\|_0 = 1$ *and* $\langle s_j, s_k\rangle_0 = 0$ *for* $j = 1, \ldots, k-1$. Note that $\langle \cdot, \cdot \rangle_0 = \langle \cdot, \cdot \rangle_{L^2(\mathcal{D})}$. Equivalently, one could define the POD basis to be the solution of the problem: *minimize*

$$\mathcal{E}(s_1, \ldots, s_K) = \sum_{n=1}^{N} \|w_n - \Pi w_n\|_0^2$$

over all possible K*-dimensional* $L^2(\mathcal{D})$*-orthonormal sets* $\{s_k(\mathbf{x})\}_{k=1}^K$ *in* V_0^h, where Πw_n is the $L^2(\mathcal{D})$-projection of w_n onto the span of the functions $\{s_k(\mathbf{x})\}_{k=1}^K$. Moreover, one can instead determine the POD basis by first solving the $N \times N$ eigenvalue problem: for $k = 1, \ldots, \widetilde{M}$,

$$\mathbb{C}\vec{a}_k = \sigma_k^2 \vec{a}_k, \qquad |\vec{a}_k| = 1, \qquad \vec{a}_\ell^T \vec{a}_k = 0 \text{ if } k \neq \ell, \quad \text{and} \quad \sigma_k \geq \sigma_{k-1} > 0, \tag{4.5}$$

then setting

$$\Phi_k(\mathbf{x}) = \sum_{n=1}^{N} \frac{1}{\sigma_k} a_{k,n} w_n(\mathbf{x}) \qquad \text{for } k = 1, \ldots, K.$$

Here, we have that the rank $\widetilde{M} \leq N$ correlation matrix $\mathbb{C}$ is defined by $\mathbb{C}_{mn} = \langle w_m, w_n \rangle_0$, and $a_{k,n}$ is the n-th component of the eigenvector $\vec{a}_k$. Note that in terms of the snapshot matrix $\mathbb{A}$ and the mass matrix $\mathbb{M}$ for the finite element basis, i.e., for $\mathbb{M}_{ij} = (\Phi_i, \Phi_j)_0$, we now have that $\mathbb{C} = \mathbb{A}^T\mathbb{M}\mathbb{A}$. This fact allows us to again use the singular value decomposition to determine the POD basis function. To this end, let $\mathbb{M} = \mathbb{S}^T\mathbb{S}$, where the $J \times J$ matrix $\mathbb{S}$ may be chosen to be a symmetric, positive definite square root of $\mathbb{M}$, i.e., $\mathbb{S} = \mathbb{M}^{1/2}$, or $\mathbb{S}$ could be a Cholesky factor, i.e., $\mathbb{S}^T = \mathbb{L}$. Then, we let $\widetilde{\mathbb{A}} = \mathbb{S}\mathbb{A}$ so that $\mathbb{C} = \mathbb{A}^T\mathbb{M}\mathbb{A} = \widetilde{\mathbb{A}}^T\widetilde{\mathbb{A}}$ and therefore $\vec{a}_k$, $k = 1, \ldots, K$, are the first K right singular vectors of $\widetilde{\mathbb{A}}$.

4.2. The POD reduced-order models. We now show how a POD basis is used to define a reduced-order model for the nonlinear stochastic PDE (3.1). For the sake of brevity, we only discuss the case for which the snapshot set is viewed as a set of finite element coefficient vectors; the case for which the snapshot set is a set of finite element functions proceeds in similar manner.

Let $\{\vec{\Phi}_k\}_{k=1}^K$ be a K-dimensional POD basis corresponding to the snapshot set $\{\vec{w}_n\}_{n=1}^N$. For each $\vec{\Phi}_k$, $k = 1, \ldots, K$, there is a finite element function

$$\Phi_k(\mathbf{x}) = \sum_{j=1}^{J} \mathbf{\Phi}_{j,k} \phi_j(\mathbf{x}) \in S_0^h, \tag{4.6}$$

where $\mathbf{\Phi}_{j,k}$ denotes the jth component of $\vec{\Phi}_k$. Let

$$U_K = \text{span}\{\Phi_k\}_{i=1}^K \subset S_0^h.$$

As will be explained in Section 5.1, the reduced basis functions satisfy homogeneous boundary conditions. We then seek a reduced basis approximation of the stochastic process field of the form

$$u^K(t, \cdot) \in U_K.$$

We determine $u^K(t,\cdot)$, $t \in I$, from the discrete problem

$$
\begin{cases}
\displaystyle\int_{\mathcal{D}} \frac{\partial u^K}{\partial t}\Phi(\mathbf{x})\mathrm{d}\mathcal{D} + \int_{\mathcal{D}} \{\nabla u^K \cdot \nabla \Phi\}\mathrm{d}\mathcal{D} \\
\qquad\qquad + \gamma \displaystyle\int_{\mathcal{D}} N(u^K(s,\mathbf{x}))\Phi(\mathbf{x})\mathrm{d}\mathcal{D} \\
\qquad\qquad = \displaystyle\int_{\mathcal{D}} \left(g(t,\mathbf{x}) + \epsilon \frac{\partial^3 \widehat{\mathbb{W}}}{\partial t \partial x_1 \partial x_2}(t,\mathbf{x};\omega) \right) \Phi(\mathbf{x})\mathrm{d}\mathcal{D} \\
\qquad u^K(0,\mathbf{x}) = 0, \text{ in } \mathcal{D} \quad \forall \Phi(\mathbf{x}) \in U_K.
\end{cases} \tag{4.7}
$$

The reduced basis approximation of the stochastic process takes the form

$$u^K(t,\cdot) = \sum_{k=1}^{K} \alpha_k(t;\omega)\Phi_k$$

and (4.7) may be expressed as

$$
\begin{cases}
\displaystyle\sum_{k=1}^{K} \frac{d\alpha_k}{dt} \int_{\mathcal{D}} \Phi_k(\mathbf{x})\Phi_j(\mathbf{x})\mathrm{d}\mathcal{D} + \sum_{k=1}^{K} \alpha_k(t) \int_{\mathcal{D}} \nabla\Phi_k \nabla\Phi_j \mathrm{d}\mathcal{D} \\
\qquad\qquad + \gamma \displaystyle\int_{\mathcal{D}} N\left(\sum_{k=1}^{K} \alpha_k(t)\Phi_k(\mathbf{x}) \right) \Phi_j \mathrm{d}\mathcal{D} \\
\qquad\qquad = \displaystyle\int_{\mathcal{D}} \left(g(t,\mathbf{x}) + \epsilon \frac{\partial^3 \widehat{\mathbb{W}}}{\partial t \partial x_1 \partial x_2}(t,\mathbf{x};\omega) \right) \Phi_j(\mathbf{x})\mathrm{d}\mathcal{D} \\
\qquad \displaystyle\sum_{k=1}^{K} \alpha_k(0;\omega)\Phi_k(\mathbf{x}) = 0, \text{ in } D,
\end{cases} \tag{4.8}
$$

for $j = 1, \ldots, K$. Equivalently, we have the system of nonlinear ordinary differential equations that determine the coefficient functions $\{\alpha_k(t;\omega)\}_{k=1}^K$:

$$
\begin{cases}
\mathbb{G}\dfrac{d}{dt}\vec{\alpha}(t;\omega) + \widetilde{\mathbb{G}}\vec{\alpha}(t;\omega) + \vec{N}\left(\vec{\alpha}(t;\omega)\right) = \vec{f}(t;\omega) \\
\vec{\alpha}(0;\omega) = \vec{\alpha}_0,
\end{cases} \tag{4.9}
$$

where the Gram matrix $\mathbb{G}$, stiffness matrix $\widetilde{\mathbb{G}}$, nonlinear vector function $\vec{N}\left(\vec{\alpha}(t;\omega)\right)$, and solution vector $\vec{\alpha}(t;\omega)$ are respectively given by

$$
\mathbb{G}_{jk} = \int_{\mathcal{D}} \Phi_k(\mathbf{x})\Phi_j(\mathbf{x})\mathrm{d}\mathcal{D}, \qquad \widetilde{\mathbb{G}}_{jk} = \int_{\mathcal{D}} \nabla\Phi_k\nabla\Phi_j\mathrm{d}\mathcal{D},
$$

$$
\vec{N}\left(\vec{\alpha}(t;\omega)\right) = \gamma \int_{\mathcal{D}} N\left(\sum_{k=1}^{K} \alpha_k(t;\omega)\Phi_k(\mathbf{x}) \right) \Phi_j \mathrm{d}\mathcal{D} \qquad \text{and} \qquad (\vec{\alpha})_k = \alpha_k(t;\omega)
$$

for $j,k = 1, \ldots, K$, while the forcing vector $\vec{f}(t;\omega)$ and initial data vector $\vec{\alpha}_0$ are respectively given by

$$
(\vec{f})_j = \int_{\mathcal{D}} \left(g(t,\mathbf{x}) + \epsilon \frac{\partial^3 \widehat{\mathbb{W}}}{\partial t \partial x_1 \partial x_2}(t,\mathbf{x};\omega) \right) \Phi_j(\mathbf{x})\mathrm{d}\mathcal{D}
$$

and

$$(\vec{\alpha}_0)_j = 0$$

for $j = 1, \ldots, K$. Unlike the matrices in a standard FEM formulation, these matrices are not sparse; but their order K is so much smaller (see Section 5) that their density is of no consequence. Another important observation is that matrices $\mathbb{G}$, $\widetilde{\mathbb{G}}$, depend only on the reduced basis functions $\{\Phi_k\}_{k=1}^K$ so that they may all be pre-computed.

4.3. The error in a reduced-order solution. At any given time t, we define the "error" $\mathfrak{E}(t)$ in a POD reduced-order solution to be the $L^2(\mathcal{D})$-norm of the difference between the *expected value* of the full finite element solution and the *expected value* of the reduced-order solution, i.e.,

$$\begin{aligned}\mathfrak{E}(t) &= \left\{ \int_{\mathcal{D}} \left(\int_\Omega u^h(t,\mathbf{x};\omega)\mathbf{P}(\mathrm{d}\omega) - \int_\Omega u^K(t,\mathbf{x};\omega)\mathbf{P}(\mathrm{d}\omega) \right)^2 \mathrm{d}\mathcal{D} \right\}^{1/2} \\ &= \left\{ \int_{\mathcal{D}} \left(\mathbf{E}(u^h(t,\mathbf{x};\omega)) - \mathbf{E}(u^K(t,\mathbf{x};\omega)) \right)^2 \mathrm{d}\mathcal{D} \right\}^{1/2} \\ &\approx \left\{ \int_{\mathcal{D}} \left(\overline{\mathbf{E}}(u^h;M) - \overline{\mathbf{E}}(u^K;M) \right)^2 \mathrm{d}\mathcal{D} \right\}^{1/2}, \end{aligned} \tag{4.10}$$

where $u^h(t,\mathbf{x};\omega)$ denotes the approximate stochastic process determined using the full finite element simulation code, and $u^K(t,\mathbf{x};\omega)$ denotes the approximate stochastic process determined by a POD reduced-order model. The expected value $\mathbf{E}(\cdot)$ is defined in Section 2. Using the standard MCFEM described in section 3.1, we approximate $\mathbf{E}(u^h)$ by sampling averages $\overline{\mathbf{E}}(u^h;M)$ where M is the number of sample realizations. We can use a similar Monte Carlo reduced-order modeling technique to approximate $\mathbf{E}(u^K)$ by $\overline{\mathbf{E}}(u^K;M)$ for the same number of sample realizations. Also of interest is the space-time error

$$\begin{aligned}\mathfrak{E}_T = \left\{ \int_0^T \mathfrak{E}^2(s)\mathrm{d}s \right\}^{1/2} &= \left\{ \int_0^T \int_{\mathcal{D}} \left(\mathbf{E}(u^h(t,\mathbf{x};\omega)) - \mathbf{E}(u^K(t,\mathbf{x};\omega)) \right)^2 \mathrm{d}\mathcal{D}\mathrm{d}s \right\}^{1/2} \\ &\approx \left\{ \int_0^T \int_{\mathcal{D}} \left(\overline{\mathbf{E}}(u^h;M) - \overline{\mathbf{E}}(u^K;M) \right)^2 \mathrm{d}\mathcal{D}\mathrm{d}s \right\}^{1/2}. \end{aligned} \tag{4.11}$$

There are two contributions to these "errors." One is due to the fact that the reduced-order model does not exactly reproduce the information contained in the snapshot set; the other to the fact that the snapshot set itself cannot exactly represent the full finite element solution.

Recall that the POD reduced bases are determined from a set of snapshots and that those bases are designed so that *most* of the information in the snapshot set is captured. But because we truncate the singular value decomposition quite early, it is clear that even if the only solutions encountered were linear combinations of snapshot vectors, there would be many such solutions which would lie partially or entirely outside the span of the reduced basis.

Even if a reduced basis could exactly capture all the information in the snapshot set, the errors (4.10) and (4.11) would not vanish because the snapshot set itself cannot exactly capture all the behaviors allowed in the full finite element space.

A snapshot cannot exactly represent even the finite element solutions used in its construction because that set consists of a time-sampling of those solutions. Also, a snapshot set represents only a discrete set of sampled values of any system parameters or boundary conditions. Strong nonlinearities in those effects can reveal that a snapshot set is inadequate for a given problem.

The analyst must therefore always keep in mind the limitations of the snapshot approach. On the other hand, it is easy to automate, and generally quite practical. It has been demonstrated many times in the literature that POD-based reduced-order models are excellent at exploiting the information contained in a snapshot set; the computational experiments reported in Section 5 provide one such example. Thus, a key to designing reduced-order models of the POD type is to ensure that the snapshot set contains sufficient information for the problems to be considered.

5. Computational experiments

We compare the use, efficiency, and accuracy of the POD-based reduced-order modeling techniques on an example. We consider a nonlinear stochastic PDE in which a perturbation parameter ϵ controls the intensity of the space-time white noise. The problem has a relatively strong cubic nonlinearity, in which the strength of the nonlinear function $N(u(t,\mathbf{x}) = u(1-u)^2$ is $\gamma = 10$. The nonlinear stochastic PDE is rewritten as follows: find $u : \bar{I} \times \mathcal{D} \to \mathbb{R}$ such that

$$
\begin{cases}
\dfrac{\partial u}{\partial t}(t,\mathbf{x}) - \Delta u(t,\mathbf{x}) + 10\, u(t,\mathbf{x})(1-u(t,\mathbf{x}))^2 \\
\qquad = e^t \sin(x_1)\cos(x_2) + \epsilon \dfrac{\partial^3 \widehat{\mathbb{W}}}{\partial t \partial x_1 \partial x_2}(t,\mathbf{x};\omega), \text{ in } I \times \mathcal{D} \\
u(t,\mathbf{x}) = 0, \text{ on } \partial\mathcal{D} \\
u(0,\mathbf{x}) = 0, \text{ in } \mathcal{D},
\end{cases}
\tag{5.1}
$$

where $\mathbf{x} = (x_1, x_2)$ and the deterministic forcing term $g(t,\mathbf{x}) = e^t \sin(x_1)\cos(x_2)$.

The Galerkin finite element method on a square grid of $J = 1089$ nodes is used in the discrete weak formulation, described in section 3.1, to obtain accurate stochastic Galerkin finite element approximations of solutions of (5.1). This choice of spatial dimension is arbitrary; however for this initial study, a relatively course grid was chosen to all us to compute multiple realizations of the stochastic example problem (5.1). The time derivative is discretized by a backward-Euler method. Newton's method is used to solve the fully discrete nonlinear stochastic PDE. Finite element solutions are used for the generation of snapshots and later for comparison with POD-based reduced-order solutions.

The snapshot solutions are generated by the finite element method applied to problem (5.1) for a particular number of realizations; each realization samples the piecewise constant white noise $\Delta\widehat{\mathbb{W}}(\cdot\,;\omega)$ with a specific perturbation parameter ϵ whose assignment is to be discussed next.

5.1. Generating snapshots. For all simulations involved in the snapshot generation process, ϵ is chosen to have the value 0.1. The snapshot vectors are determined by the following procedure. First, for $k = 1, \ldots, \widetilde{K} = 10$ realizations and $t \in I = (0,1)$, a finite element approximation is determined $\sum_{j=1}^{J} w(t;\omega_k)\phi(\mathbf{x})$ of the solution of (5.1), where J denotes the dimension of the finite element space S_0^h, and $\{\phi_j\}_{j=1}^{J}$ denotes the basis functions for that space. This is the approximate stochastic process used to generate the snapshots. For $S = 200$ and $P = 10$, the $N = S \times P = 2000$ snapshot vectors

$$
\vec{w}_n = \vec{w}_{sp} = \begin{pmatrix} w_1(t_s;\omega_p) \\ w_2(t_s;\omega_p) \\ \vdots \\ w_J(t_s;\omega_p) \end{pmatrix}, \quad \text{for } s = 1, \ldots, S, \text{ and } p = 1, \ldots, P
\tag{5.2}
$$

are then determined for P realizations of (5.1). For each realization $p = 1, \ldots, P$, the solution is started impulsively, and evaluated at 200 equally spaced time values t_s, $s = 1, \ldots, 200$, ranging from $t = 0$ to $T = 1$, for a total of 2000 snapshots. The time interval used for sampling snapshots is the same used for the time discretization of the nonlinear SPDE (5.1). The snapshot vectors $\{\vec{w}_n\}_{n=1}^N$ correspond to the snapshot functions

$$\mathbf{w}_n(\mathbf{x}) = \mathbf{w}_{sp}(\mathbf{x}) = \sum_{j=1}^{J} w_j(t_s; \omega_p)\phi_j(\mathbf{x}) \quad \text{for } n = 1, \ldots, N.$$

It is sometimes convenient to modify the snapshot set $\{\vec{w}_n\}_{n=1}^N$ to satisfy certain boundary conditions. In this case, the snapshot vectors naturally satisfy the Dirichlet homogeneous boundary conditions. It might also seem relevant to compute the sample average of the P realizations and use the resulting S snapshot vectors rather than the complete N snapshot vectors in the reduced-order model. In the next section, it is explained why this approach was not employed.

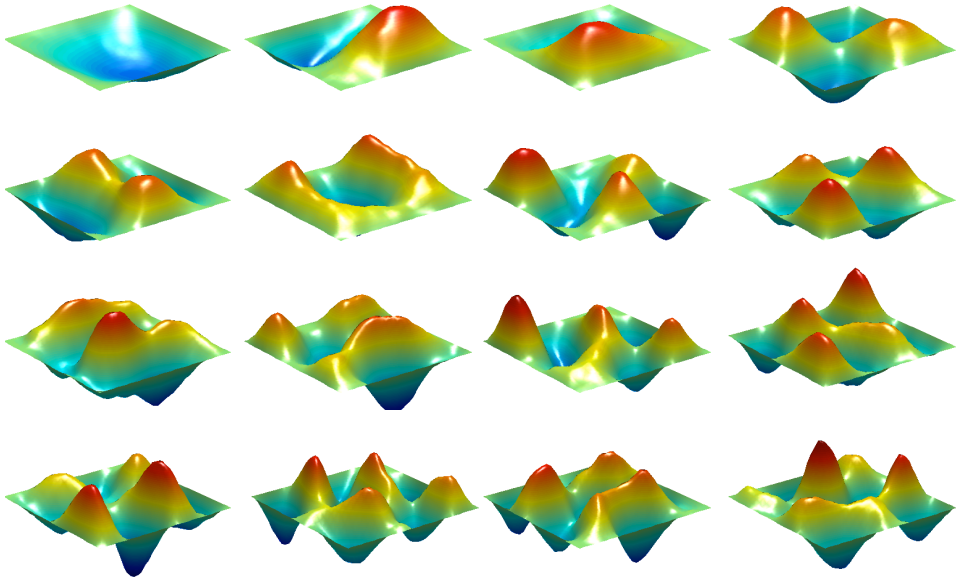

FIGURE 2. The POD reduced basis of cardinality 16 for the nonlinear stochastic problem 5.1.

5.2. POD reduced bases. POD reduced bases corresponding to the snapshot set $\{\vec{w}_n\}_{n=1}^N$ are determined as described in Section 4.1. As described in the previous section, each POD basis function satisfies zero Dirichlet boundary conditions on the boundary $\delta\mathcal{D}$. The elements of a K-dimensional POD basis constitute the first K elements of all POD bases of dimension greater that K. For the snapshot set determined as described in Section 5.1, the 16-dimensional POD basis functions are displayed in Figure 2 and the first 16 singular values of the corresponding snapshot matrix are listed in Table 1. In the context of POD-based reduced-order modeling, one expects the singular values to decrease rapidly, indicating that a low-dimension POD basis can capture most of the information in the snapshot set. This behavior cannot, of course, be universal, but it has been observed in many examples. In our particular problem we observe from Table 1 and Figure 5.2, that

1	34.0387	5	8.8536	9	6.4498	13	5.5122
2	13.0477	6	8.4762	10	6.1230	14	4.8172
3	11.7138	7	7.3131	11	5.8013	15	4.7471
4	9.7154	8	7.1571	12	5.5966	16	4.6712

TABLE 1. The first 16 singular values of the snapshot matrix for the example problem (5.1).

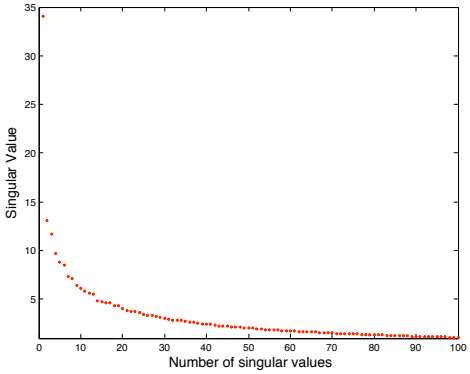

FIGURE 3. The first 100 singular values of the snapshot matrix for the example problem (5.1).

the singular values of the corresponding snapshot matrix decay rather slowly to zero. However, we shall show in section 5.5 that the POD-based reduced-order models for the nonlinear SPDE still perform adequately for the approximation of ensemble averages of finite element solutions, rather than for the approximate finite element solutions themselves; this is the usual case for POD-basis reduced-order models. That is, a "small-dimensional" POD basis can still be sufficient if our primary interest is approximating the expected value of finite element solutions, and not the approximation of a particular realization.

Note that if one computes the sample average of the P realizations and uses the resulting S snapshot vectors rather than the complete N snapshot vectors, the resulting singular values decay at the same rate. Therefore, the smaller snapshot set does not provide any extra information or improvement over our reduced-order calculation.

5.3. Determining POD-based reduced-order approximations. Given a perturbation parameter ϵ and a particular $\omega \in \Omega$, the K-dimensional system of nonlinear ordinary differential equations (4.9) is used to determine reduced-order solutions of the example problem (5.1). Approximate solutions of the system of ordinary differential equations (4.9) can be determined using an ODE solver of appropriate order. The computations described here use the finite element type assembly, described in section 3, for the considerably smaller K-dimensional system.

The vectors and matrices appearing in the system (4.9) depend only on the choice of reduced basis, so that once a POD basis is determined as described in section 5.2 it can be reused for different choices of ϵ and ω. This is a major advantage of POD-based reduced-order models, where the primary interest is the approximation of the expected value $\mathbf{E}(u^h(\cdot\,;\omega)$. Similar to the MCFEM described in section 3.1,

we again use a Monte Carlo sampling method for the reduced-order model. That is, given the number of realizations $M \in \mathbb{N}_+$ we sample iid realizations of the piecewise constant white noise $\Delta\widehat{\mathbb{W}}(\cdot\,;\omega_k)$ for $k = 1, \ldots, M$ and find $u^K(\cdot\,;\omega)$ satisfying (4.7). The quantity $\mathbf{E}(u^h)$ is then approximated by the sampling average:

$$\overline{\mathbf{E}}(u^K; M) = \frac{1}{M}\sum_{k=1}^{M} u^K(\cdot\,;\omega_k) \tag{5.3}$$

To illustrate the effectiveness of the low-dimensional, POD-based reduced-order models, we employ several perturbation parameters ϵ and several different choices for the dimension of the reduced bases. Note that the set $\{\omega_p\}_{p=1}^{P}$ used to generate the snapshot vectors $\{\vec{w}_n\}_{n=1}^{N}$ is distinct from the set $\{\omega_k\}_{k=1}^{M}$ used to calculate the sample average (5.3).

5.4. Perturbation parameters for POD-based reduced-order models. The specific choices used for ϵ in the reduced-order simulation are given as follows. For $M = 1000$ realizations, we compute the sampling average $\overline{\mathbf{E}}(u^K; M)$, described by (5.3), using several different cases: $\epsilon = 0, 0.01, 0.05, 0.1, 0.5, 1$. In each case, the reduced-order solution u^K satisfies (4.7).

It is worth noting something about the six perturbation parameters ϵ used in these computational experiments: For all cases except $\epsilon = 0.1$, the perturbation parameter is different from the parameter used to generate the snapshots. This is, of course, how one wants to use a reduced-order model: generate a reduced basis using snapshots determined from finite element simulations for some specific choice of data for the example problem (5.1), and then solve the reduced-order model for a variety of different data. For those cases, the reduced-order simulations are carried out over the time interval $[0, 1]$, which is the same time interval used to generate the snapshots.

5.5. Computational results. For all six cases, full finite element solutions employing thousands of unknowns are determined so that they may be compared to the POD-based reduced-order solutions for the same data. Specifically, for the comparisons, we use the measures $\mathfrak{E}(t)$ and $\mathfrak{E}_T$ defined in (4.10) and (4.11), respectively.

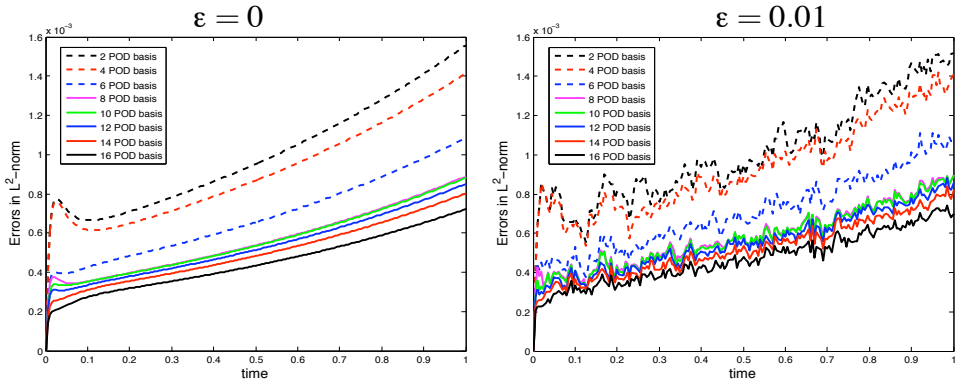

FIGURE 4. $\mathfrak{E}(t)$ for the POD-based reduced-order models with *epsilon* $= 0$ and $\epsilon = 0.1$. The plots are on the same scale indicated the effects on the error by introducing the perturbation parameter ϵ into the ROM.

In Figure 6, plots of $\mathfrak{E}(t)$ versus the time t are provided for each of the six test problems described in Section 5.4. In each plot, results are displayed for eight values of the POD basis K, ranging from 2 to 16. Each plot has been scaled separately, to exhibit the drop in error as K increases. To consider the effect of ϵ, we also provide, in Figure 4, a pan of plots drawn to the same scale, for $\epsilon = 0$ and $\epsilon = 0.01$. A comparison of these plots demonstrates the effect of introducing noise into the system (1.1), while also suggesting how well the mean of the reduced-order solution still approximates the mean of the finite element solution of the deterministic PDE. Both plots indicate that the error grows with ϵ but can be reduced by increasing K. Obviously, for a given K, by increasing ϵ, the approximation error $\mathfrak{E}(t)$ will generally be larger.

For the example problem (5.1), an examination of Figure 6 shows that very low-dimensional POD-based reduced-order models are quite effective at approximating the expected value of the full finite element solutions; even for bases of dimension less than 10, the "error" $\mathfrak{E}(t)$ is small. As the perturbation parameter increases, though, a larger number of basis vectors are required to control the error $\mathfrak{E}(t)$. It should be noted that for small perturbation parameters, $0 < \epsilon \leq 0.01$, the error $\mathfrak{E}(t)$ follows the error for the case $\epsilon = 0$, with the obvious stochastic effects present. The results also suggest that, for this problem, increasing the order of the reduced basis beyond about $K = 10$ produced very little further improvement in accuracy. This conclusion can also be inferred from Table 2 where the space-time "error" $\mathfrak{E}_T$ versus K is listed. There is a much slower reduction in the error as K increases from 10 to 16 than the change from 2 to 10.

K	$\epsilon = 0$	$\epsilon = 0.01$	$\epsilon = 0.05$	$\epsilon = 0.1$	$\epsilon = 0.5$	$\epsilon = 1$
2	3.17e-02	3.19e-02	3.90e-02	5.07e-02	1.25e-01	2.08e-01
4	3.03e-02	3.06-02	3.72e-02	4.79e-02	1.15e-01	1.89e-01
6	2.61e-02	2.66e-01	3.44e-02	4.54e-02	1.09e-01	1.76e-01
8	2.37e-02	2.42e-02	3.25e-02	4.34e-02	1.04e-01	1.67e-01
10	2.36e-02	2.41e-02	3.18e-02	4.22e-02	9.99e-02	1.60e-01
12	2.31e-02	2.36e-02	3.10e-02	4.11e-02	9.96e-02	1.53e-01
14	2.24e-02	2.29e-02	3.01e-02	4.00e-02	9.37e-02	1.48e-01
16	2.12e-02	2.17e-02	2.93e-02	3.91e-02	9.13e-02	1.44e-01

TABLE 2. $\mathfrak{E}_T$ for the POD-based reduced-order models vs. the dimension K of the reduced basis space for the six test cases.

Finally, Figure 6 and Table 2 show that POD-based reduced-order models have the ability to approximate the expected value of full finite element solutions by solving a very small dimensional system. This is also evident from observing Figure 5 which plots the approximate expected value $\overline{\mathbf{E}}(u^h)$ using the full FEM versus the approximate expected value $\overline{\mathbf{E}}(u^K)$ using the reduced-order model with 2, 8 and 16 POD vectors at times $t = 0, 0.25, 0.5, 0.75$ and 1. From this plot we see that as the dimension K increases from 2 to 16 the quality of the approximation improves dramatically.

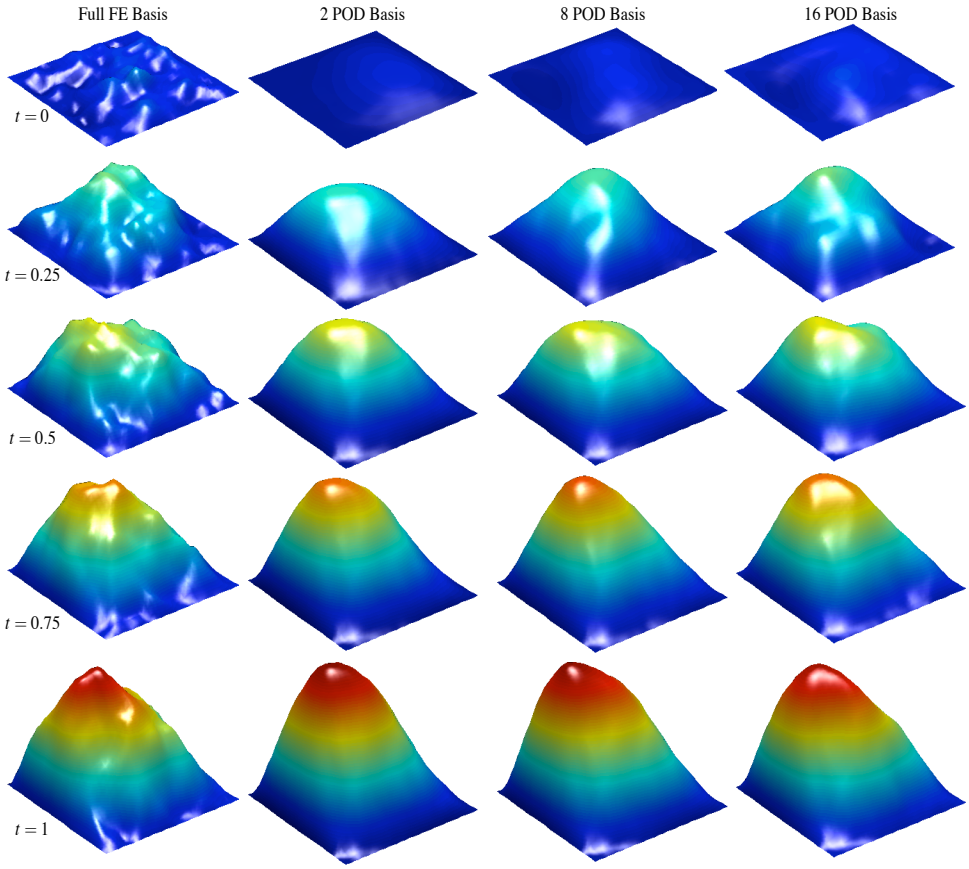

FIGURE 5. The approximate expected value $\overline{\mathbf{E}}(u^h)$, using the full FEM versus the approximate expected value $\overline{\mathbf{E}}(u^K)$ using the ROM with 2, 8 and 16 POD vectors at times $t = 0, 0.25, 0.5, 0.75$ and 1. All plots are generated for the case $\epsilon = 0.1$.

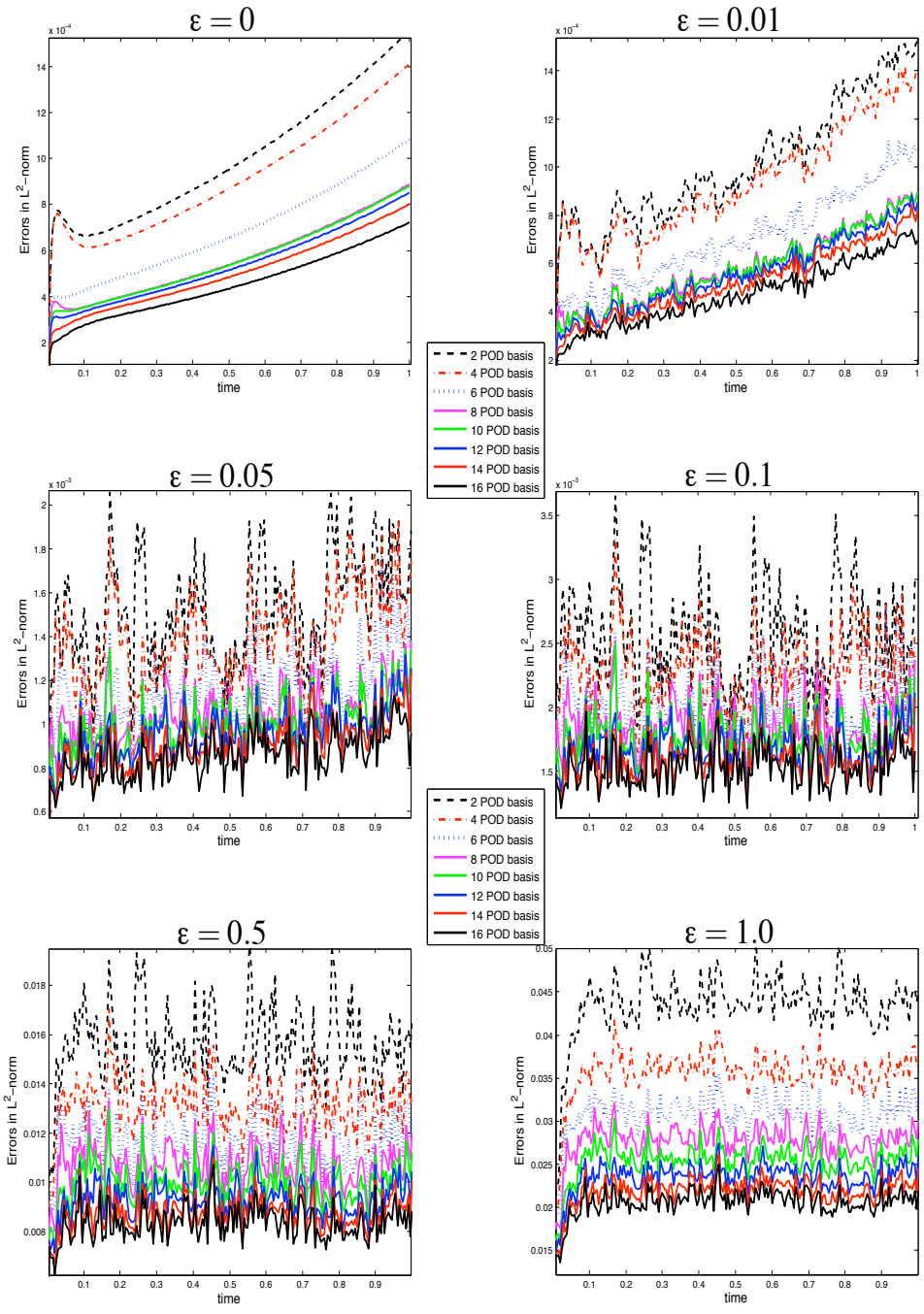

FIGURE 6. $\mathfrak{E}(t)$ for the POD-based reduced-order models for Cases 1-6. As the perturbation parameter ϵ increases from 0 to 1.0, the scale of the plots is adjusted to clearly display the error behavior.

6. Concluding remarks

We saw in section 4.1 that snapshots can be viewed either as finite element coefficient vectors or as finite element functions. The net effect of taking the latter view is the appearance of the finite element mass matrix $\mathbb{M}$ in, e.g., (4.5). Although handling the appearance of the mass matrix does not add a significant cost to the determination of a reduced basis, it also does not appreciably improve the performance of the reduced-order model. For this reason, in section 5.5, we only provided results based on viewing snapshots as coefficient vectors.

The results given in Section 5.5 suggest that POD-based reduced-order modeling can be very effective in approximating the expected value of solutions of a nonlinear stochastic PDE driven by space-time additive white noise. It is therefore appropriate to briefly examine the cost of these POD-based reduced-order models. If one settles on a reduced-order modeling technique that relies on the generation of snapshots, then one only needs to discuss the production of a reduced-order basis when comparing the cost of such a procedures. That is, regardless of the type of reduced-order model employed, one must certainly "pay the price" of computing a snapshot set. The expense of extracting the reduced order basis from the snapshot set is minuscule compared to the cost of generating the snapshot set itself.

POD methods have attracted much research interest in recent years as an inexpensive means of simulating deterministic PDEs. To our knowledge, little work has been done on extending this method to the field of stochastic PDEs, and yet this is a field of study which seems ideal for this approach, given the need to consider a vast ensemble of solutions. We hope that this work invites further inquiry by others into a relatively open area.

There are many worthwhile problems to consider in both linear and nonlinear stochastic PDEs. For instance, multiplicative noise, which provides greater correlation, could be applied to the coefficients of the equation or the forcing functions. Studies of these cases may lead to a better understanding of the errors that occur when approximating ensemble averages of solutions by a reduced-order model. Such investigations will increase the understanding, interest and application of these methods for the analysis of the stochastic dynamics of linear and nonlinear problems of practical interest [18, 24, 55–58].

Acknowledgments

The third author wish to thank Professor Max Gunzburger for his guidance and insight in the area of reduced-order modeling. This research was supported by the School of Computational Science at Florida State University.

References

[1] E. J. Allen and S. J. Novosel and Z. Zhang, Finite Element and Difference Approximation of Some Linear Stochastic Partial , *Stochastics Rep.* **64**, 1998, 117-142.

[2] E. Alós and S. Bonaccorsi, Stochastic Partial Differential Equations with Dirichlet White-Noise Boundary Conditions, *Ann. I. H. Poincaré* **38**, 2002, 152-154.

[3] N. Aubry and W. Lian, and E. Titi, Preserving symmetries in the proper orthogonal decomposition, *SIAM J. Sci. Comp.* **14**, 1993, 483-505.

[4] I. Babuśka and K. M. Liu, On Solving Stochastic Initial-Value Differential Equations, *Mathematical Models and Methods in Applied Sciences*, 2001, 1-37.

[5] I. Babuśka and R. Tempone and G. Zouraris, Solving Elliptic Boundary Value Problems with Uncertain Coefficients by the Finite Element method: the Stochastic Formulation, *Comput. Methods Appl. Mech. Engrg.* **194**, 2005, 1251-1294.

[6] I. Babuśka and R. Tempone and G. Zouraris, Galerkin Finite Element Approximations of Stochastic Elliptic Partial Differential Equations, *SIAM J. Numeric. Anal.* **42**, 2004, 800-825.

[7] G. Berkooz, P. Holmes and J. Lumley, The proper orthogonal decomposition in the analysis of turbulent flows, *Ann. Rev. Fluid. Mech.* **25**, 1993, 539-575.
[8] G. Berkooz and E. Titi, Galerkin projections and the proper orthogonal decomposition for equivariant equations, *Phys. Let. A* **174** 1993, 94-102.
[9] R. Buckdahn and E. Pardoux, Monotonicity methods for white noise driven quasilinear SPDEs, in Diffusion Processes and Related Problems in Analysis, *I, M. Pinsky, ed.*, 1990, 219-233.
[10] J. Burkardt and M. Gunzburger and H. C. Lee, POD and CVT-based Reduced-order Modeling of Navier-Stokes flows, 2004, to appear
[11] J. Burkardt and M. Gunzburger and H. C. Lee, Centroidal Voronoi Tessellation-Based Reduced-Order Modeling of Complex Systems, 2003, to appear
[12] E. Christensen and M. Brons, and J. Sorensen, Evaluation of proper orthogonal decomposition-based decomposition techniques applied to parameter-dependent nonturbulent flows, *SIAM J. Sci. Comp.* **21**, 2000, 1419-1434.
[13] R. Dalang and C. Mueller, Some Nonlinear SPDE's that are Second Order in Tiime, *Electronic Journal of Probability* **8**, 2003, 1-21.
[14] G. Da Prato and L. Tubaro, Stochastic Partial Differential Equations and Applications, *Longman Scientific and Technical.*, 1992.
[15] G. Da Prato and J. Zabczyk, Stochastic Equations in Infinite Dimensions, *Cambridge University Press.*, 1992.
[16] A. M. Davie and J. G. Gaines, Convergence of Numerical Schemes for the Solution of Parabolic Stochastic Partial Differential Equatioins, *Mathematics of Computation.* **70**, 2000, 121-134.
[17] A. Deane and I. Kevrekidis and G. Karniadakis and S. Orszag, Low-dimensional models for complex geometry flows: applications to grooved channels and circular cylinders, *Phys. Fluids A* **3**, 1991, 2337-2354.
[18] J. Deang and Q. Du and M. Gunzburger, Thermal fluctuations of superconducting vortices,, *Phy. Rev. B.*, **64**, 2001, 52506-52510.
[19] M. K. Deb and I. Babuśka and J. T. Oden, Solution of stochastic partial differential equations using Galerkin finite element, *Comput. Methods Appl. Mech. Engrg.* **190**, 2001, 6359-6372.
[20] Q. Du and T. Zhang, Numerical Approximation of Some Linear Stochastic Partial Differential Equations Driven by Special Additive Noises, *SIAM J. Numer. Anal.* **40**, 1993, 1421-1445.
[21] Q. Du and M. Gunzburger, Model reduction by proper orthogonal decomposition coupled with centroidal Voronoi tessellation, *Proc. Fluids Engineering Division Summer Meeting*, FEDSM2002-31051, ASME, 2002.
[22] Q. Du and M. Gunzburger, Centroidal Voronoi tessellation based proper orthogonal decomposition analysis, *Proc. 8th Conference on Control of Distributed Parameter Systems*, Birkhauser, Basel, 2002. 137-150.
[23] Q. Du and M. Gunzburger and L. Ju, Meshfree, probabilistic determination of points, sets and support regions for meshless computing, *Comput. Meth. Appl. Mech. Engrg.* **191**, 2002, 1349-1366.
[24] W. G. Faris and G. Jona-Lasino, Large Fluctuations for a Nonlinear Heat Equation with Noise, *J. Phys. A:Math Gen.* **18**, 1982, 3025-3055.
[25] M. Graham and I. Kevrekidis, Pattern analysis and model reduction: Some alternative approaches to the Karhunen-Lóeve decomposition, *Comp. Chem. Engng.* **20**, 1996, 495-506.
[26] I. Gyongy, Lattice Approximations of Stochastic Quasi-Linear Parabolic Partial Differential Equations Driven by Space-Time White Noise II, *Potential Analysis.* **11**, 1999, 1-37.
[27] I. Gyongy and T. Martinez, On the Approximation of Solutions of Stochastic Differential Equations of Elliptic Type, 2003, to appear.
[28] P. Holmes and J. Lumley and G. Berkooz, *Turbulence, Coherent Structures, Dynamical Systems and Symmetry*, Cambridge University Press, Cambridge, 1996.
[29] P. Holmes and J. Lumley and G. Berkooz and J. Mattingly and R. Wittenberg, Low-dimensional models of coherent structures in turbulence, *Phys. Rep.* **287**, 1997, 337-384.
[30] C. Johnson, Numerical Solution of Partial Differential Equations by the Finite Element Method, *Cambridge University Press.*, 1994.
[31] P. E. Kloeden and E. Platen, Numerical Solution Stochastic Differential Equations , *Spring-Verlag.*, 1992.

[32] K. Kunisch and S. Volkwein, Control of Burger's equation by a reduced order approach using proper orthogonal decomposition, *JOTA* **102**, 1999, 345-371.
[33] K. Kunisch and S. Volkwein, Galerkin proper orthogonal decomposition methods for parabolic problems, *Spezialforschungsbereich F003 Optimierung und Kontrolle,* Projektbereich Kontinuierliche Optimierung und Kontrolle, Bericht Nr. 153, Graz, 1999.
[34] J. Lumley, *Stochastic Tools in Turbulence*, Academic, New York, 1971.
[35] H. G. Matthies and A. Keese, Galerkin Methods for Linear and Nonlinear Elliptic Stochastic Partial Differential Equations, 2003, to appear.
[36] L. Mytnik, Stochastic Partial Differential Equation Driven by Stable Noise, *Probab. Theory Relat. Fields.* **123**, 2002, 157-201.
[37] D. Nagy, Modal representation of geometrically nonlinear behavior by the finite element method, *Comput. & Struct.* **10**, 683 (1979).
[38] A. K. Noor, Recent advances in reduction methods for nonlinear problems, *Comput. & Struct.* **13**, 31 (1981).
[39] A. K. Noor and C.M. Anderson and J.M. Peters, Reduced basis technique for collapse analysis of shells, *AAIA J.* **19**, 393 (1981).
[40] A. K. Noor and J.M. Peters, Tracking post-linit-paths with reduced basis technique, *Comput. Methods Appl. Mech. Eng.* **28**, 217 (1981).
[41] A. K. Noor, Recent advances in reduction methods for nonlinear problems, *Comput. & Struc.* **13**, 1981, 31-44.
[42] B. Øksendal, Stochastic Differential Equations. An Introduction with Applications , *Spring-Verlag.*, fifth edition, 1998.
[43] H. M. Park and D. Cho, Low dimensional modeling of flow reactors, Int. J. Heat Mass Transf. **39**, 1996, 3311-3323.
[44] H. M. Park and J. S. Chung A sequential method of solving inverse natural convection problems. Inverse Problems 18 (2002), no. 3, 529–546.
[45] H. M. Park and Y. D. Jang Control of Burgers equation by means of mode reduction. Internat. J. Engrg. Sci. 38 (2000), no. 7, 785–805
[46] H. M. Park and J. H. Lee Solution of an inverse heat transfer problem by means of empirical reduction of modes. Z. Angew. Math. Phys. 51 (2000), no. 1, 17–38
[47] H. M. Park and M. W. Lee An efficient method of solving the Navier-Stokes equations for flow control. Internat. J. Numer. Methods Engrg. 41 (1998), no. 6, 1133–1151
[48] H. M. Park and W. J. Lee A new numerical method for the boundary optimal control problems of the heat conduction equation. Internat. J. Numer. Methods Engrg. 53 (2002), no. 7, 1593–1613
[49] J. S. Peterson, The reduced basis method for incompressible viscous flow calculations, *SIAM J. Sci. Stat. Comput.* **10**. 777 (1989).
[50] M. Rathinam and L. Petzold, A new look at proper orthogonal decomposition, to appear.
[51] M. Rathinam and L. Petzold, Dynamic iteration using reduced order models: A method for simulation of large scale modular systems, to appear.
[52] S. Ravindran, Proper orthogonal decomposition in optimal control of fluids, *Int. J. Numer. Meth. Fluids* **34**, 2000, 425-448.
[53] S. Ravindran, Reduced-order adaptive controllers for fluid flows using POD, J. Sci. Comput. 15 (2000), no. 4, 457–478.
[54] J. Rodríguez and L. Sirovich, Low-dimensional dynamics for the complex Ginzburg-Landau equations, *Physica D* **43**, 1990, 77-86.
[55] J. Sancho, J. Garcia-Ojalvo and H. Guo, Non-equilibrium Ginzburg-Landau model driven by colored noise, *Phys. D.* **113**, 1998, 331-337.
[56] T. Shardlow, Numerical Simulation of Stochastic PDEs for Excitable Media, *Journal of Computational and Applied Mathematics.* **175**, 2005, 429-446.
[57] T. Shardlow, Weak Convergence of a Numerical Method For a Stochastic Heat Equation, *BIT Numerical Mathematics.* **43**, 2003, 179-193.
[58] T. Shardlow, Nucleation of Waves in Excitable Media by Noise, *Multiscal Model Simul.* **3**, 2004, 151-167.
[59] L. Sirovich, Turbulence and the dynamics of coherent structures, I-III, *Quart. Appl. Math.* **45**, 1987, 561-590.
[60] N. Smaoui and D. Armbruster, Symmetry and the Karhunen-Loève analysis, *SIAM J. Sci. Comput.* **18**, 1997, 1526-1532.
[61] I. M. Sobol, A Primer for Monte Carlo Method, *CRC Press.* 1994.

[62] S. Volkwein, Optimal control of a phase field model using the proper orthogonal decomposition, *ZAMM* **81**, 2001, 83-97.
[63] S. Volkwein, Proper orthogonal decompositionand singular value decomposition, *Spezialforschungsbereich F003 Optimierung und Kontrolle*, Projektbereich Kontinuierliche Optimierung und Kontrolle, Bericht Nr. 153, Graz, 1999.
[64] Y. Yan, The Finite Element Method for a Linear Stochastic Parabolic Partial Differential Equation Driven by Additive Noise, 2003, to appear.
[65] Y. Yan, Semidiscrete Galerkin Approximation for a Linear Stochastic Parabolic Partial Differential Equation Driven by an Additive Noise, 2002, to appear.

School of Computational Sciences, Florida State University, Tallahassee, FL, 32306-4120, USA
E-mail: burkardt@scs.fsu.edu
URL: http://www.scs.fsu.edu/∼burkardt

School of Computational Sciences, Florida State University, Tallahassee, FL, 32306-4120, USA
E-mail: gunzburg@scs.fsu.edu
URL: http://www.scs.fsu.edu/∼gunzburg

School of Computational Sciences and Department of Mathematics, Florida State University, Tallahassee, FL, 32306-4120, USA
E-mail: webster@scs.fsu.edu
URL: http://www.scs.fsu.edu/∼webster